

ASPECTS RELATED TO THE USE OF THE MOHR-COULOMB MODEL IN SEISMIC SLOPE STABILITY ANALYSES

VICTOR MATEI PETRESCU - assistant, Technical University of Civil Engineering, Bucharest
e-mail: matei@ppm.ro

Abstract: The finite element method is increasingly used in the analysis of geotechnical problems, including problems related to the stability of slopes. This paper considers the use of the Mohr-Coulomb constitutive model for analysing slope failures under plane strain conditions. A method is proposed to compensate some limitations of the finite elements, so that the failure of a slope can be modelled with high enough accuracy. An analysis example, which illustrates the effects of this method, is also presented. A free and open source finite element analysis program developed by the author of this article, and which can be downloaded from <http://matgts.sf.net>, was used.

Rezumat: Metoda elementului finit este utilizată din ce în ce mai mult în analiza problemelor din domeniul geotehnicii și implicit a problemelor legate de stabilitatea taluzurilor și versanților. Articolul de față se referă la utilizarea modelului Mohr-Coulomb pentru analiza cedării taluzurilor, în condițiile stării plane de deformații. Este propusă o metodă pentru compensarea unor limitări ale elementelor finite, astfel încât cedarea unui taluz să poată fi modelată cu o precizie suficient de bună. Este prezentat de asemenea un exemplu de calcul care ilustrează efectele metodei respective. S-a utilizat un program de calcul prin metoda elementului finit, liber și cu sursă deschisă, elaborat de către autorul acestui articol și care poate fi descărcat de la adresa <http://matgts.sf.net>.

Keywords: finite, element, method, failure, plane, strain

1. INTRODUCTION

In slope stability analyses, the finite element method has several advantages compared to simplified methods based on limit equilibrium. For instance, it eliminates the need for simplifying assumptions concerning the shape of the failure surface or the interaction forces between slices. However, the finite elements and the constitutive models used also have their limitations, which are especially important in modelling the failure of soils. This paper proposes and exemplifies a method for improving the results of slope stability analyses. Rectangular finite elements with linear shape functions, 8 degrees of freedom and some modifications which compensate for the limitations of the linear shape functions (Petrescu, 2012)^[1] are used in the analyses presented here, as well as a computer program developed by the author of this article. The program is available at the address <http://matgts.sf.net> under the terms of the GNU GPL license, version 3 (<http://www.gnu.org>).

2. MOHR-COULOMB MODEL

In the case of plane strain conditions, Equations (1) and (2) can be used for expressing the behaviour of an isotropic linear elastic material.

$$\begin{pmatrix} \dot{\sigma}_x \\ \dot{\sigma}_y \\ \dot{\tau}_{xy} \end{pmatrix} = \frac{E}{(1-2\nu)(1+\nu)} \begin{pmatrix} 1-\nu & \nu & 0 \\ \nu & 1-\nu & 0 \\ 0 & 0 & \frac{1-2\nu}{2} \end{pmatrix} \begin{pmatrix} \dot{\epsilon}_x \\ \dot{\epsilon}_y \\ \dot{\gamma}_{xy} \end{pmatrix} = [D^e] \begin{pmatrix} \dot{\epsilon}_x \\ \dot{\epsilon}_y \\ \dot{\gamma}_{xy} \end{pmatrix} \quad (1)$$

$$\sigma_z = \sigma_2 = \nu \cdot (\sigma_x + \sigma_y) \quad (2)$$

The Mohr-Coulomb model is characterised by a yield function, (3), and a plastic potential function, (4). To maintain consistency with the linear elastic model, the normal stresses will be considered positive in the case of tension and negative in the case of compression.

$$F(\sigma) = \sigma_1 - \sigma_3 - 2 \cdot c \cdot \cos \phi + (\sigma_1 + \sigma_3) \cdot \sin \phi \quad (3)$$

$$P(\sigma) = \sigma_1 - \sigma_3 + (\sigma_1 + \sigma_3) \cdot \sin \psi \quad (4)$$

where:

σ_1, σ_3 - maximum and minimum principal stresses;

ϕ - internal friction angle;

ψ - dilatancy angle ($\psi = \arcsin(\alpha)$, where α is the dilatancy coefficient);

c - cohesion.

Under plane strain conditions, Equation (2) is also valid in the case of the Mohr-Coulomb model, because the yield and plastic potential functions don't depend on σ_2 . Therefore, $\sigma_2 = \sigma_z$ will be omitted from the following equations. When $F(\sigma) < 0$, the material is considered to have an elastic behaviour, described by (1) and (2). When $F(\sigma) = 0$, the material is considered to have failed and another matrix must be determined instead of $[D^e]$. The equations used for determining that matrix, $[D^p]$, are (5) ... (11).

$$\{\dot{\sigma}\} = [D^e] \cdot \{\dot{\epsilon}_e\} = [D^e] \cdot (\{\dot{\epsilon}\} - \{\dot{\epsilon}_p\}) \quad (5)$$

where:

$\{\dot{\epsilon}\}, \{\dot{\epsilon}_e\}, \{\dot{\epsilon}_p\}$ - time derivatives of total, elastic and plastic strains;

Equation (5) expresses the fact that stresses are modified only by elastic strains.

$$\dot{F}(\sigma) = \sum_{i=1}^n \left(\frac{\partial F}{\partial \sigma_i} \cdot \dot{\sigma}_i \right) = \left(\frac{\partial F}{\partial \sigma} \right)^T \cdot \{\dot{\sigma}\} = 0 \quad (6)$$

According to (6), F remains constant and therefore doesn't become greater than 0.

Equations (5) and (6) are not sufficient for determining the plastic constitutive matrix and other hypotheses are necessary. In case of the Mohr-Coulomb model, these are based on the plastic potential function, $P(\sigma)$, as shown in (7).

$$\{\dot{\epsilon}_p\} = \Lambda \cdot \left\{ \frac{\partial P}{\partial \sigma} \right\} \quad (7)$$

Equations (5), (6) and (7) can be used for the determination of Equations (8), (9) and (10).

$$\dot{F}(\sigma) = \left\{ \frac{\partial F}{\partial \sigma} \right\}^T \cdot [D^e] \cdot \left(\{\dot{\epsilon}\} - \Lambda \cdot \left\{ \frac{\partial P}{\partial \sigma} \right\} \right) = 0 \quad (8)$$

$$\Lambda = \frac{\left\{ \frac{\partial F}{\partial \sigma} \right\}^T \cdot [D^e] \cdot \{\dot{\epsilon}\}}{\left\{ \frac{\partial F}{\partial \sigma} \right\}^T \cdot [D^e] \cdot \left\{ \frac{\partial P}{\partial \sigma} \right\}} \quad (9)$$

$$\{\dot{\sigma}\} = [D^e] \cdot \{\dot{\epsilon}\} - \frac{\left\{ \frac{\partial F}{\partial \sigma} \right\}^T \cdot [D^e] \cdot \{\dot{\epsilon}\}}{\left\{ \frac{\partial F}{\partial \sigma} \right\}^T \cdot [D^e] \cdot \left\{ \frac{\partial P}{\partial \sigma} \right\}} \cdot [D^e] \cdot \left\{ \frac{\partial P}{\partial \sigma} \right\} = [D^p] \cdot \{\dot{\epsilon}\} \quad (10)$$

Thus, the plastic constitutive matrix, $[D^p]$, is expressed in the form given by Equation (11).

$$[D^p] = [D^e] - \frac{[D^e] \cdot \left\{ \frac{\partial P}{\partial \sigma} \right\} \cdot \left\{ \frac{\partial F}{\partial \sigma} \right\}^T \cdot [D^e]}{\left\{ \frac{\partial F}{\partial \sigma} \right\}^T \cdot [D^e] \cdot \left\{ \frac{\partial P}{\partial \sigma} \right\}} \quad (11)$$

The partial derivatives of the yield and plastic potential functions can be calculated according to Equations (12) ... (20).

$$\sigma_{1,3} = \frac{\sigma_x + \sigma_y}{2} \pm \sqrt{\left(\frac{\sigma_x - \sigma_y}{2} \right)^2 + \tau_{xy}^2} \quad (12)$$

$$\frac{\partial \sigma_1}{\partial \sigma_x} = \frac{\partial \sigma_3}{\partial \sigma_y} = \frac{1}{2} + \frac{\sigma_x - \sigma_y}{4 \cdot \sqrt{\left(\frac{\sigma_x - \sigma_y}{2} \right)^2 + \tau_{xy}^2}} \quad (13)$$

$$\frac{\partial \sigma_1}{\partial \sigma_y} = \frac{\partial \sigma_3}{\partial \sigma_x} = \frac{1}{2} - \frac{\sigma_x - \sigma_y}{4 \cdot \sqrt{\left(\frac{\sigma_x - \sigma_y}{2} \right)^2 + \tau_{xy}^2}} \quad (14)$$

$$\frac{\partial \sigma_1}{\partial \tau_{xy}} = -\frac{\partial \sigma_3}{\partial \tau_{xy}} = \frac{\tau_{xy}}{\sqrt{\left(\frac{\sigma_x - \sigma_y}{2}\right)^2 + \tau_{xy}^2}} \quad (15)$$

$$\frac{\partial F}{\partial \sigma_1} = 1 + \sin \phi \quad ; \quad \frac{\partial F}{\partial \sigma_3} = -1 + \sin \phi \quad (16)$$

$$\frac{\partial P}{\partial \sigma_1} = 1 + \sin \psi \quad ; \quad \frac{\partial P}{\partial \sigma_3} = -1 + \sin \psi \quad (17)$$

$$\frac{\partial F}{\partial \sigma_x} = \frac{\partial F}{\partial \sigma_1} \cdot \frac{\partial \sigma_1}{\partial \sigma_x} + \frac{\partial F}{\partial \sigma_3} \cdot \frac{\partial \sigma_3}{\partial \sigma_x} \quad ; \quad \frac{\partial P}{\partial \sigma_x} = \frac{\partial P}{\partial \sigma_1} \cdot \frac{\partial \sigma_1}{\partial \sigma_x} + \frac{\partial P}{\partial \sigma_3} \cdot \frac{\partial \sigma_3}{\partial \sigma_x} \quad (18)$$

$$\frac{\partial F}{\partial \sigma_y} = \frac{\partial F}{\partial \sigma_1} \cdot \frac{\partial \sigma_1}{\partial \sigma_y} + \frac{\partial F}{\partial \sigma_3} \cdot \frac{\partial \sigma_3}{\partial \sigma_y} \quad ; \quad \frac{\partial P}{\partial \sigma_y} = \frac{\partial P}{\partial \sigma_1} \cdot \frac{\partial \sigma_1}{\partial \sigma_y} + \frac{\partial P}{\partial \sigma_3} \cdot \frac{\partial \sigma_3}{\partial \sigma_y} \quad (19)$$

$$\frac{\partial F}{\partial \tau_{xy}} = \frac{\partial F}{\partial \sigma_1} \cdot \frac{\partial \sigma_1}{\partial \tau_{xy}} + \frac{\partial F}{\partial \sigma_3} \cdot \frac{\partial \sigma_3}{\partial \tau_{xy}} \quad ; \quad \frac{\partial P}{\partial \tau_{xy}} = \frac{\partial P}{\partial \sigma_1} \cdot \frac{\partial \sigma_1}{\partial \tau_{xy}} + \frac{\partial P}{\partial \sigma_3} \cdot \frac{\partial \sigma_3}{\partial \tau_{xy}} \quad (20)$$

Although Equations (12) ... (20) can be used for determining matrix $[D^p]$, it is more useful to calculate the plastic constitutive matrix which relates the time derivatives of stresses and strains in the directions of the principal stresses, $[A]$, and then rotate it, according to Equations (21) ... (23), because this permits the introduction of a shear stiffness reduction coefficient, s , which is used to compensate for some limitations of the finite elements.

It can be shown that $a_{1,3} = a_{2,3} = a_{3,1} = a_{3,2} = 0$ and $a_{3,3} = \frac{E}{2 \cdot (1 + \nu)}$. In Equation (21), matrix $[A]$ appears already modified and coefficient $a_{3,3}$ is multiplied with s .

$$\begin{pmatrix} \dot{\sigma}_3 \\ \dot{\sigma}_1 \\ \dot{\tau}_{31} \end{pmatrix} = [A] \cdot \begin{pmatrix} \dot{\epsilon}_3 \\ \dot{\epsilon}_1 \\ \dot{\gamma}_{31} \end{pmatrix} = \begin{pmatrix} a_{1,1} & a_{1,2} & 0 \\ a_{2,1} & a_{2,2} & 0 \\ 0 & 0 & s \cdot \frac{E}{2 \cdot (1 + \nu)} \end{pmatrix} \cdot \begin{pmatrix} \dot{\epsilon}_3 \\ \dot{\epsilon}_1 \\ \dot{\gamma}_{31} \end{pmatrix} \quad (21)$$

$$[D^p] = [C]^T \cdot [A] \cdot [C] \quad (22)$$

$$[C] = \begin{pmatrix} \cos^2 \theta & \sin^2 \theta & \sin \theta \cdot \cos \theta \\ \sin^2 \theta & \cos^2 \theta & -\sin \theta \cdot \cos \theta \\ -2 \cdot \sin \theta \cdot \cos \theta & 2 \cdot \sin \theta \cos \theta & \cos^2 \theta - \sin^2 \theta \end{pmatrix} \quad (23)$$

$$\begin{pmatrix} \dot{\sigma}_x \\ \dot{\sigma}_y \\ \dot{\tau}_{xy} \end{pmatrix} = [D^p] \cdot \begin{pmatrix} \dot{\epsilon}_x \\ \dot{\epsilon}_y \\ \dot{\gamma}_{xy} \end{pmatrix} \quad (24)$$

where θ is the angle shown in Figure 1 and calculated according to (25).

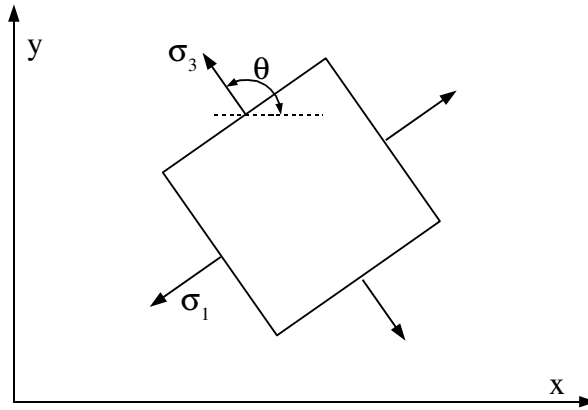


Figure 1 - Principal stresses (σ_1, σ_3)

$$\sigma_x > \sigma_y \rightarrow \theta = \frac{\arctg\left(\frac{2 \cdot \tau_{xy}}{\sigma_x - \sigma_y}\right)}{2} + \frac{\pi}{2} ; \quad \sigma_x \leq \sigma_y \rightarrow \theta = \frac{\arctg\left(\frac{2 \cdot \tau_{xy}}{\sigma_x - \sigma_y}\right)}{2} \quad (25)$$

A graphical representation of the relation between σ_1 and σ_3 when $F(\sigma) = 0$ is shown in Figure 2.

The Mohr-Coulomb model does not account for the absence of the tensile strength of soils, so it can't be used without modifications for modelling the behaviour of a soil subjected to tension in a realistic way. In the computer program mentioned in this article, when $s = \frac{\sigma_1 + \sigma_3}{2} > c \cdot \text{ctg} \phi$, the constitutive matrix used is defined by Equation (26).

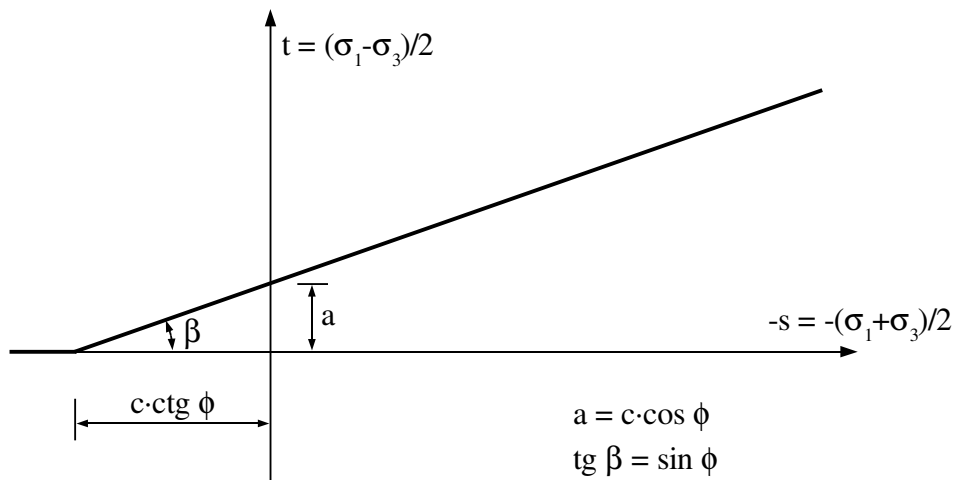


Figure 2 - Graphical representation of the failure condition

$$\begin{pmatrix} \dot{\sigma}_x \\ \dot{\sigma}_y \\ \dot{\tau}_{xy} \end{pmatrix} = \frac{E}{(1-2\nu)(1+\nu)} \cdot \begin{pmatrix} 0.5 & 0.5 & 0 \\ 0.5 & 0.5 & 0 \\ 0 & 0 & 0 \end{pmatrix} \cdot \begin{pmatrix} \dot{\epsilon}_x \\ \dot{\epsilon}_y \\ \dot{\gamma}_{xy} \end{pmatrix} = [D^f] \cdot \begin{pmatrix} \dot{\epsilon}_x \\ \dot{\epsilon}_y \\ \dot{\gamma}_{xy} \end{pmatrix} \quad (26)$$

3. ANALYSIS EXAMPLE

Three pseudo-static analyses were performed for the model in Figure 3, with the purpose of determining the horizontal critical acceleration, using the finite element method, as well as Bishop's simplified method (Bishop, 1955)^[2]. The parameters of the model were: $L = 10$ m, $H = 10$ m, $\gamma = 20$ KN/m³, $\phi = 10^\circ$, $c = 30$ kPa. The finite element analyses were performed for 2 values of coefficient s from Equation (21): $s = 1$ and $s = 0.05$.

In the finite element analyses, the load was applied in 2 phases:

1. Vertical load determined by the weight of the material;
2. Horizontal load, equal to the weight of the material multiplied with a coefficient k_H , whose value was increased until the failure of the slope was reached.

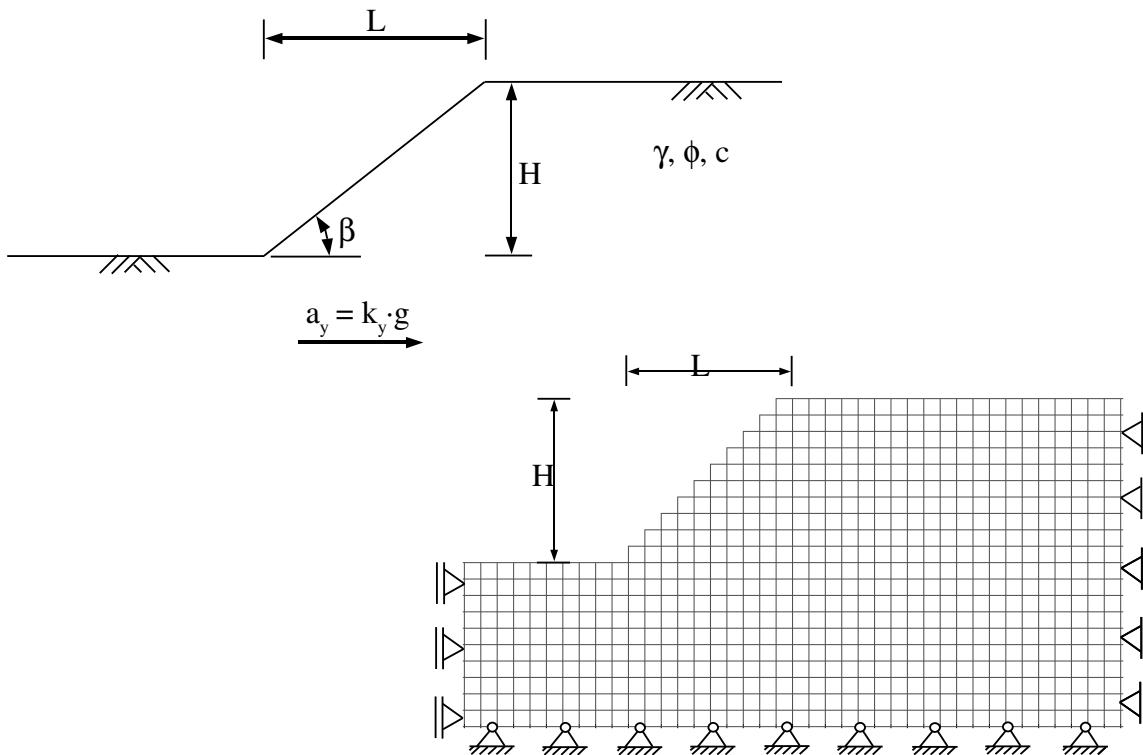


Figure 3 - Model used in analyses

The critical values of coefficient k_H obtained in the 3 analyses were:

- Bishop's simplified method: $k_y = 0.15$;
- Finite element analysis, $s = 0.05$: $k_y \approx 0.16$;
- Finite element analysis, $s = 1$: $k_y > 0.17$;

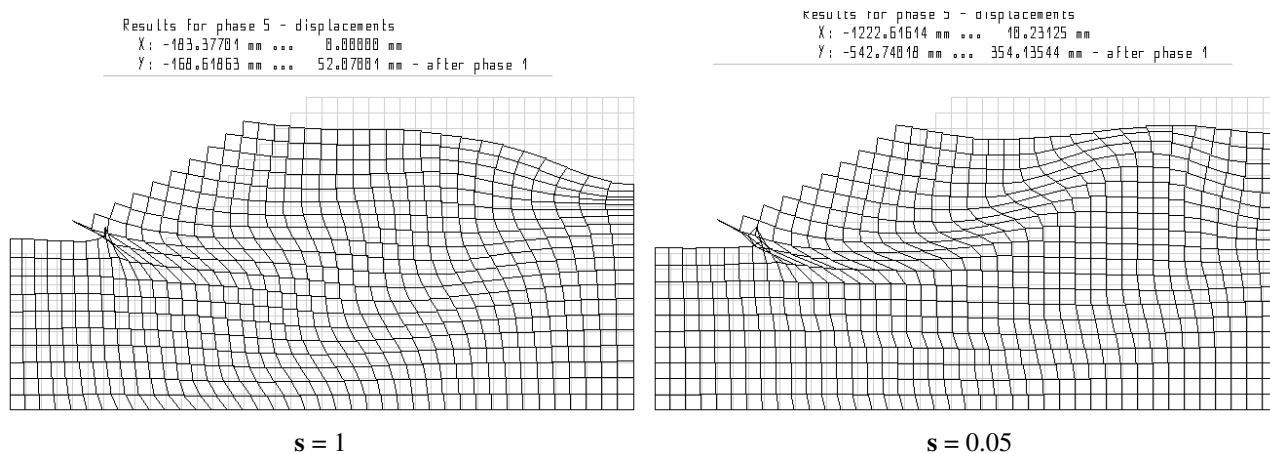


Figure 4 - Displacements of the model in Figure 3, for a coefficient $k_H = 0.17$

4. CONCLUSIONS

As can be seen from the results of the analyses presented here, the value of the coefficient s from Equation (21) has a very important effect on the behaviour of the model. When s was equal to 1, as it would normally be in the case of the Mohr-Coulomb model, the failure of the slope was not modelled realistically and the value of the critical coefficient k_y was much greater than that obtained through Bishop's simplified method. This happened because in general, adjacent elements develop different failure planes and therefore block each other's deformations. By using a coefficient $s = 0.05$, the stiffnesses of the failed elements were not only eliminated along the failure planes, but also reduced in all directions, which allowed much more realistic results to be obtained. In this case ($s = 0.05$), both the failure surface and the critical coefficient (k_y) were close to those obtained with Bishop's simplified method, which demonstrates the efficiency of the method proposed in this article in producing good results when rectangular elements with linear deformations are used. Compared to higher order elements, these elements have the advantage of fewer degrees of freedom, which leads to fewer equations.

References

- [1] Petrescu, V.M. - Aspecte privind utilizarea elementelor finite plane în calculul deformațiilor, Buletinul Științific al Universității Tehnice de Construcții București, 2012
- [2] Bishop A. - The Use of the Slip Circle in the Stability Analysis of Slopes, Geotechnique 5, 1955
- [3] Potts D. M., Zdravković L. - Finite Element Analysis in Geotechnical Engineering, Thomas Telford Publishing, London, 1999